A latent Gaussian Markov random field model for spatio-temporal rainfall disaggregation

David J. Allcroft and Chris A. Glasbey

Biomathematics & Statistics Scotland, Edinburgh, UK

Summary. Rainfall data are often collected at coarser spatial scales than required for input into hydrology and agricultural models. We therefore describe a spatio-temporal model which allows multiple imputation of rainfall at fine spatial resolutions, with a realistic dependence structure in both space and time and with the total rainfall at the coarse scale consistent with that observed. The method involves the transformation of the fine-scale rainfall to a thresholded Gaussian process which we model as a Gaussian Markov random field (GMRF). Gibbs sampling is then used to efficiently generate realisations of rainfall at the fine scale. Results compare favourably with previous, less elegant methods.

Keywords: Disaggregation; Gaussian Markov random field (GMRF); Gibbs sampling; Latent Gaussian model; Rainfall

1. Introduction

Many models in hydrology and agriculture require meteorological variables as inputs, however the available data will rarely be of the desired form. For example, rainfall data is generally collected at coarser spatial scales than required, hence the need for a spatio-temporal model which will allow multiple imputation of rainfall at fine scales, which are consistent with the observed totals at the coarse scale. There is a growing literature on spatio-temporal models, simply because there is a great need for them, with many datasets being both spatial and temporal. Some approaches combine geostatistical methods in space with time series models, for example Mardia et al. (1998) combine kriging with the Kalman filter and Wikle et al. (2001) develop a fully Bayesian hierarchical model. Alternatively, for data on a lattice, space-time autoregressive moving average (STARMA) models can be defined (see, for example, Pfeifer and Deutsch, 1980; Cressie, 1991, pp. 449). In this paper we use a Gaussian Markov random field (GMRF), sometimes also called a conditional autoregressive model (see, for example, Besag and Kooperberg, 1995; Cressie, 1991, pp. 433). These are a sub-class of Gaussian fields which have a Markov property, i.e. non-adjacent locations are conditionally independent, and therefore Gibbs sampling can be used for efficient simulation. Rainfall is non-Gaussian, but by suitable transformation we demonstrate that it can be modelled as a thresholded Gaussian variable. We can then formulate the process as a spatio-temporal GMRF and simulate disaggregations by Gibbs sampling.

To illustrate our approach we consider 12 hours of hourly data from the Arkansas-Red Basin River Forecast Center website, `http://www.srh.noaa.gov/abrfc`. This particular sequence of data sees a storm moving across the region. Chandler et al. (2000) modelled the data at 8km$\times$8km resolution, then aggregated to 5$\times$5 blocks and proceeded to disaggregate. We do likewise. Fig. 1 shows one hour of data at both fine (75×150 values) and coarse (15×30) resolutions. The approach of Chandler et al. (2000) was limited to binary presence/absence data and was complex, involving a combination of transition probabilities, regression relationships and Markov random fields. Subsequently, Mackay et al. (2001)

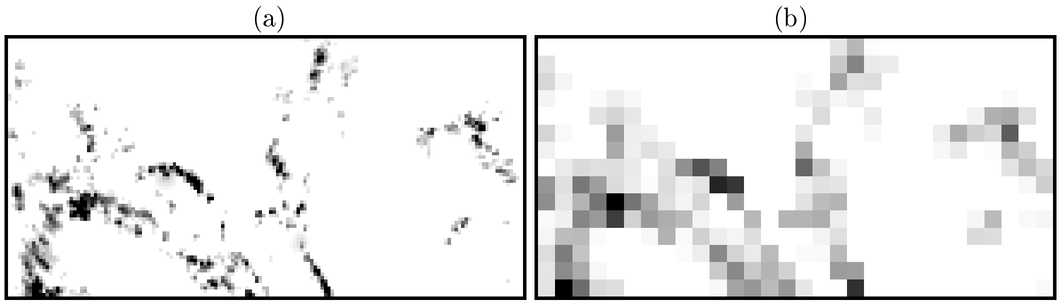

Fig. 1. One of 12 hours of data, at (a) fine and (b) coarse resolution. Rainfall intensities are displayed as shades of grey of increasing darkness; white indicates zero rainfall and the darkest shade over 30mm.

extended this by simulating values for rainfall intensity and allocating them to wet locations. Similar two-stage approaches have been used previously for rainfall modelling, for example Stern and Coe (1984) use a (non-stationary) Markov chain for rainfall occurrence and a gamma distribution for the rainfall intensities. Hughes et al. (1999) use a hidden Markov model instead. We see our latent variable approach as more elegant, being able to take account of rainfall occurrence and intensity in a single variable. Use of latent variables was also suggested by Sansó and Guenni (1999), who worked in a Bayesian framework, and Guillot (1999), who terms his approach *meta-Gaussian*. Previously, another popular approach to modelling rainfall was to use point processes (see, for example, Rodriguez-Iturbe et al., 1988).

In Section 2 we describe the method for fitting a Gaussian Markov random field to the data described above. Section 3 then demonstrates how the disaggregation is performed and shows results. Finally, Section 4 is a short discussion.

2. Model

To fit a Gaussian Markov random field, we assume the empirical correlations of the observed data to be the correlation function of a Gaussian field and then proceed as if we are approximating a Gaussian random field by a GMRF (Rue and Tjelmeland, 2002). The first step is therefore to estimate the correlation of the observed data. In our case however we have the extra preliminary step of estimating the transformation from the rainfall variable to the thresholded latent Gaussian variable. Then it is the correlation of this latent Gaussian variable to which we fit the GMRF. It is worth noting firstly the need to fit a model to the correlation structure — simply using the estimated correlation coefficients themselves would not describe a valid process. Secondly, an alternative to fitting a GMRF would be to model the dependence with some correlation model, e.g. a Matern form (Cressie, 1991, p. 85), however because our task here is disaggregation, the GMRF formulation is the most convenient, because of the ease of conditional simulation. We now therefore describe each of the three modelling stages in turn: rainfall transformation, correlation estimation and, finally, GMRF parameter estimation.

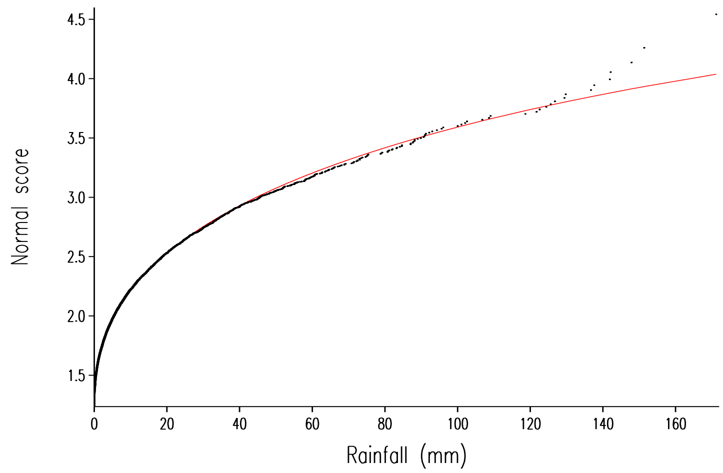

Fig. 2. Normal probability plot for 12 hours of data (·), and fitted values $f(r)$ (—).

2.1. Rainfall transformation

We seek a monotonic function to transform the rainfall to a latent Gaussian variable, such that when rain is observed, the variable takes a value above a threshold (α_0), and when no rain is observed, the variable takes a censored value below the threshold. As noted by Glasbey and Nevison (1997), a power transformation is not quite adequate to achieve normality, hence we use a quadratic function of the power-transformed rainfall. So for each location (i, j) in space at time t, we transform the rainfall (in 1/100mm), r_{ijt}, to the Gaussian variable, y_{ijt}, by

$$y = f(r) = \begin{cases} \alpha_0 + \alpha_1 r^\gamma + \alpha_2 r^{2\gamma} & \text{if} \quad r > 0, \\ * & \text{otherwise,} \end{cases} \tag{1}$$

dropping the subscripts for clarity. Here, $*$ is used to denote a censored value: $y = * \iff y \leq \alpha_0$, corresponding to the locations for which $r = 0$. This function also has the advantage of being analytically invertible, which will be important later. Parameters can be estimated by numerically minimising the sum of squares of differences between y and expected normal scores. Although maybe not fully efficient, the large amount of data makes this unimportant. Fig. 2 shows the normal probability plot of the twelve hours of data, with the least squares fit of (1), with $\alpha = (1.236, 0.04990, -0.0001610)$ and $\gamma = 0.4411$. The fit is seen to be good, except for rain levels above 140mm, but as only five of the 135000 values were in this range, this is not a cause for concern. Although the transformation is quadratic, the maximum occurs at $r = (-\alpha_1/2\alpha_2)^{1/\gamma}$, here corresponding to 923mm rain, and so the function is monotonic for the range we consider.

2.2. Estimation of correlation

The correlation of the GMRF cannot be estimated directly, as for dry locations, the Gaussian variable is censored. Therefore we take the approach of Durban and Glasbey (2001) and estimate the correlation at lag (k, l, s), denoted $\hat{\rho}_{kls}$, by maximisation of

$\sum_{ijt} \log p(y_{ijt}, y_{i-k,j-l,t-s})$. The pairwise probabilities, p, take one of three forms depending on whether neither, one or both of the locations is dry and hence the latent Gaussian variable is censored:

$$p(y_{ijt}, y_{i-k,j-l,t-s}) = \begin{cases} \Phi_2(\alpha_0, \alpha_0; \rho) & \text{if } y_{ijt} = y_{i-k,j-l,t-s} = * \\ \phi(y_{ijt}) \ \Phi\left(\frac{\alpha_0 - \rho y_{ijt}}{\sqrt{1-\rho^2}}\right) & \text{if only } y_{i-k,j-l,t-s} = * \\ \phi_2(y_{ijt}, y_{i-k,j-l,t-s}; \rho) & \text{otherwise.} \end{cases}$$

Here, ϕ and Φ are the probability density function and cumulative distribution function, respectively, for a standard univariate Gaussian distribution, and ϕ_2 and Φ_2 are the corresponding functions for the standard bivariate Gaussian distribution, i.e.

$$\phi_2(y_1, y_2; \rho) = \frac{1}{2\pi(1-\rho^2)^{1/2}} \exp\left[-\frac{1}{2(1-\rho^2)}({y_1}^2 - 2\rho y_1 y_2 + {y_2}^2)\right]$$

and

$$\Phi_2(a_1, a_2; \rho) = \int_{y_1=-\infty}^{a_1} \int_{y_2=-\infty}^{a_2} \phi_2(y_1, y_2; \rho) dy_1 dy_2.$$

Table 1 shows a small subset of the estimated correlations; higher lag correlations were also estimated. For time lag $s = 0$, we show the half-plane representing all distinct spatial directions; for time lag $s = 1$, distinct directions now fill the whole plane. We also show the correlations in time at spatial lag $(k, l) = (0, 0)$, up to temporal lag $s = 5$.

It might be anticipated that prevailing wind direction would produce an anisotropic spatial correlation structure, and indeed from Table 1 it can be seen that the correlation is more persistent in a north-west/south-east direction than south-west/north-east, due to bands of rain typically being aligned in the former direction. However, for the purpose of model-fitting, it was decided that the overall pattern was sufficiently similar in all directions for spatial isotropy to be assumed. Hence estimates at common distances were averaged, and these averages used in the subsequent model fitting.

2.3. Estimation of GMRF

The Gaussian Markov random field we consider is parameterised by the precision matrix Q and has likelihood

$$l \propto \exp\left[-\frac{1}{2} y' Q y\right].$$

For simplicity, we assume a torus wrap-round of the $n_i \times n_j \times n_t$ spatio-temporal locations, indexed $i = 0, \ldots, n_i - 1, j = 0, \ldots, n_j - 1, t = 0, \ldots, n_t - 1$. Q has a zero-pattern structure such that $Q_{ijt,kls} = 0$ unless locations (i, j, t) and (k, l, s) are *neighbours* (see Rue and Tjelmeland, 2002, for many more properties). We write the parameters of the GMRF as θ, where $\theta_{kls} = Q_{000,kls}$, and so θ_{kls} is non-zero only if the point (k, l, s) is in the neighbourhood of the reference point $(0, 0, 0)$. Fig. 3 shows the set of parameters θ for a spatio-temporal neighbourhood of size $5 \times 5 \times 3$. The reference point here is in the centre of the array at time lag $s = 0$ and all the empty locations shown will be filled by the corresponding parameters, assuming isotropy.

In fitting the GMRF we will need to compute the expected correlations, given θ. This can be done *via* two 3-D Fourier transforms. So to calculate ρ_{kls}, the expected correlation

Table 1. Estimates of correlation $\hat{\rho}_{kls}$ for spatio-temporal lags (k, l, s), expressed as percentages.

	Spatial correlation at time lag $s = 0$										
$k \setminus l$	-5	-4	-3	-2	-1	0	1	2	3	4	5
0						**100**	**89**	**75**	**65**	**59**	**54**
1	50	56	62	71	82	**90**	85	75	66	60	55
2	47	52	57	64	71	**76**	76	71	65	60	55
3	43	47	52	58	63	**66**	68	66	62	58	54
4	40	43	47	51	55	**59**	61	60	58	55	52
5	37	39	43	46	49	**52**	54	55	54	52	49
	Spatial correlation at time lag $s = 1$										
$k \setminus l$	-5	-4	-3	-2	-1	0	1	2	3	4	5
-5	42	43	45	45	45	**43**	42	40	38	36	34
-4	44	46	48	49	49	**48**	46	44	42	40	37
-3	45	48	51	53	54	**53**	52	49	46	44	41
-2	45	49	52	56	58	**59**	58	55	52	49	45
-1	46	49	53	57	61	**64**	63	60	56	53	50
0	**45**	**49**	**53**	**58**	**63**	**68**	**67**	**64**	**60**	**56**	**53**
1	43	47	52	57	62	**67**	67	65	61	58	54
2	40	44	49	53	58	**61**	63	64	61	58	55
3	37	41	45	49	53	**56**	59	60	59	57	53
4	34	37	41	45	48	**51**	54	56	56	54	51
5	32	34	37	40	43	**46**	49	51	51	51	48
	Temporal correlation at spatial lag $(k, l) = (0, 0)$										
s	0	1	2	3	4	5					
	100	**68**	**42**	**31**	**24**	**17**					

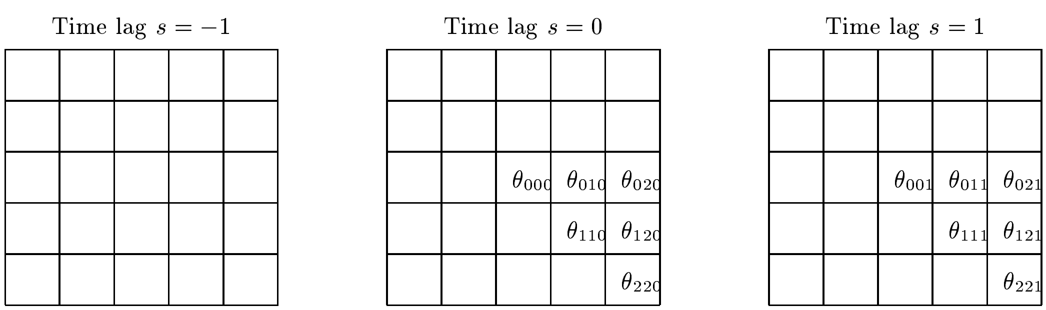

Fig. 3. Parameters θ to be estimated for a GMRF with spatio-temporal neighbourhood of size $5 \times 5 \times 3$. All remaining cells shown are completed with the given parameters assuming isotropy.

at spatio-temporal lag (k, l, s), we firstly obtain eigenvalues

$$q_{ijt} = \sum_{k=0}^{n_i-1} \sum_{l=0}^{n_j-1} \sum_{s=0}^{n_t-1} Q_{000,kls} \exp\left\{-2\pi\iota\left(\frac{ik}{n_i} + \frac{jl}{n_j} + \frac{ts}{n_t}\right)\right\},$$

for $i = 0, \ldots, n_i - 1, j = 0, \ldots, n_j - 1, t = 0, \ldots, n_t - 1$. Then we obtain covariances

$$\gamma_{kls} = \frac{1}{n_i n_j n_t} \sum_{i=0}^{n_i-1} \sum_{j=0}^{n_j-1} \sum_{t=0}^{n_t-1} \frac{1}{q_{ijt}} \exp\left\{2\pi\iota\left(\frac{ik}{n_i} + \frac{jl}{n_j} + \frac{ts}{n_t}\right)\right\},$$

for $k = 0, \ldots, n_i - 1, l = 0, \ldots, n_j - 1, s = 0, \ldots, n_t - 1$, and finally correlations are given by $\rho_{kls} = \gamma_{kls}/\gamma_{000}$.

The correlations can be computed on any size torus that is large enough to allow the correlation to die away sufficiently before wrap-round occurs; the model is then valid for any other sufficiently large grid. To ensure spatial isotropy, we fit on a torus for which $n_i = n_j$ $(= 256)$ and, as the correlation in time dies away more quickly, taking $n_t = 64$ is sufficient. Restricting the torus dimensions to powers of two makes the fast Fourier transform algorithms as efficient as possible.

Besag and Kooperberg (1995) fitted a GMRF to a covariance structure using the Kullback-Leibler discrepancy, however Rue and Tjelmeland (2002) demonstrate how this method can result in undesirable correlation outside the neighbourhood. They instead propose matching the observed and expected correlation functions, ensuring that, in terms of correlation and variance at least, a better overall fit is obtained. We follow their example and estimate the GMRF parameters by weighted least squares on the correlations, minimising

$$\sum_k \sum_l \sum_s \frac{1}{k^2 + l^2 + s^2} (\rho_{kls} - \hat{\rho}_{kls})^2, \tag{2}$$

where ρ is the expected correlation and $\hat{\rho}$ the observed correlation. The weighting factor here is analogous to that used by Rue and Tjelmeland (2002). There, in two dimensions, the weights are inversely proportional to the circumference of a circle with the given distance as radius, and here, in three dimensions, our weights are inversely proportional to the surface area of a sphere with the given distance as radius. Hence we are effectively correcting for the increasing numbers of sample values at increasing distances and in both cases, approximately equal weighting is given to all distances.

The minimisation of (2) is constrained, as we need all $q_{ijt} > 0$ to ensure that the variance matrix is positive definite and hence describes a valid process. We follow the approach of Rue and Tjelmeland (2002) and use an unconstrained simplex-based algorithm, adding a penalty if any eigenvalues are non-positive. Only correlations up to lag $(20, 20, 3)$ were included in the fitting. This was decided to be adequate, as the correlation has decayed sufficiently by this point to be such that inclusion of higher lags makes negligible difference to the estimates obtained.

Fig. 4 illustrates the fit obtained with the $5 \times 5 \times 3$ neighbourhood of Fig. 3. Table 2 shows the parameter estimates for the illustrated fit. As in Rue and Tjelmeland (2002), to aid interpretation, these have been converted to the quantities $1/\sqrt{\theta_{000}}$ and $-\theta_{kls}/\theta_{000}$, corresponding to the conditional standard deviation and conditional correlations, respectively. θ_{000} is not estimated explicitly — it is fixed at 1 in the optimisation and then scaled to fit the variance. Note that much more accuracy than that displayed in Table 2 is necessary to

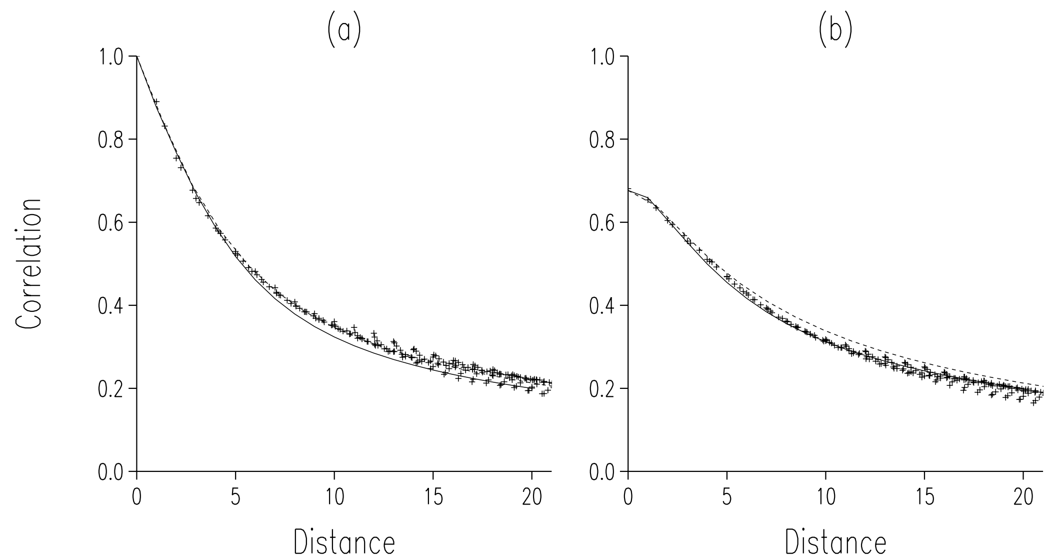

Fig. 4. Sample $\hat{\rho}$ and fitted ρ correlation of GMRF; (a) at time lag 0, (b) at time lag 1; (+) sample correlation, (—) fitted correlation along rows and columns; (- - -) fitted correlation along diagonals.

Table 2. Coefficients for the fitted GMRF. The value for $(0, 0, 0)$ is the conditional standard deviation, $1/\sqrt{\theta_{000}}$; the rest are conditional correlations, $-\theta_{kls}/\theta_{000}$.

	Time lag $s = 0$			*Time lag* $s = 1$		
	0	1	2	0	1	2
0	0.3118	0.2343	−0.0364	−0.0124	0.0401	−0.0258
1		0.0481	0.0254		0.0004	−0.0211
2			−0.0481			0.0312

recover the quoted correlation coefficients. Rue and Tjelmeland (2002) comment that these conditional correlations tend not to display any logical pattern and are hence not easy to interpret. Therefore direct specification of a model by its conditional correlations is not recommended.

The choice of neighbourhood size $5 \times 5 \times 3$ is arbitrary and might be thought to be fairly small for our example, which has relatively long correlation length. However the ability of GMRFs to achieve a good fit to a long range correlation with only a small neighbourhood is one of their more surprising and often useful features. Other neighbourhood sizes were investigated — inspection of plots similar to Fig. 4 showed one of size $3 \times 3 \times 3$ (5 parameters) to give a substantially worse fit, and one of size $7 \times 7 \times 5$ (29 parameters) to produce no noticeable improvement. Additionally, this larger neighbourhood proved unstable to fit.

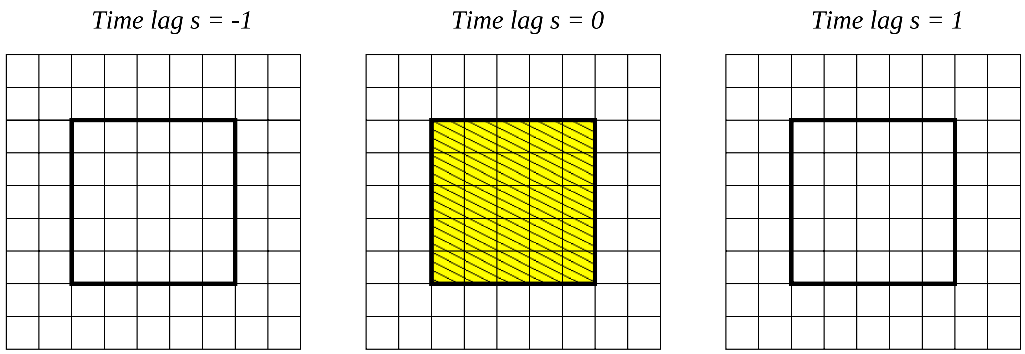

Fig. 5. Full set of locations (y_B) involved in the updating of the 5×5 block highlighted (y_A).

3. Disaggregation

We generate realisations of rainfall at the fine scale using Gibbs sampling. Starting from a configuration in which rainfall is allocated uniformly within blocks (Fig. 1b), we update 5×5 blocks such that the total rainfall within that block agrees, within measurement error, to the observed total.

Let the vector y_A be the set of 25 locations in the block to be updated and y_B be the vector of locations not conditionally independent of y_A, i.e. locations which have a non-zero entry in the precision matrix with at least one of the locations in y_A. We can write

$$\begin{pmatrix} y_A \\ y_B \end{pmatrix} \sim \mathrm{MVN}\left(\begin{pmatrix} 0 \\ 0 \end{pmatrix}, \begin{pmatrix} Q_{AA} & Q_{AB} \\ Q_{BA} & Q_{BB} \end{pmatrix}^{-1}\right),$$

and the distribution of y_A conditional on all other locations can be written $y_A |\, y_{-A} = y_A |\, y_B$. This distribution is also multivariate normal and can be conveniently expressed in terms of the precision matrix Q:

$$y_A |\, y_B \sim \mathrm{MVN}\left(-Q_{AA}^{-1} Q_{AB} y_B,\ Q_{AA}^{-1}\right). \tag{3}$$

Fig. 5 shows the set of locations that need to be taken into account for the updating of each block of 5×5 sites. For the given neighbourhood size, the number of locations in y_B is $3 \times (9 \times 9) - 25 = 218$. Since we are working on a torus, the neighbourhood size and shape is always the same and so the conditional variance needs to be calculated only once. Each conditional mean is calculated with a single matrix multiplication and so the whole simulation is computationally efficient. To weaken the wrap-round effect of the torus, we add onto the $75 \times 150 \times 12$ lattice a border of width 75 spatially and 12 temporally. This is an adequate size to allow the correlations to die away sufficiently.

We need to ensure that the total rainfall within each block is close to that observed. If the transformation (1) was linear, it would be easy to sample y_A conditional on its sum being a constant (see, for example Rue, 2001). However, r is related to y by a non-linear transformation and there is no simple method for simulation conditional on the sum of these back-transformed values being constant. Noting that the rainfall data is derived from radar and adjusted using rain gauge data, it seems reasonable to assume that there will be some estimation error here and therefore it is sufficient, and in fact more realistic, to just get agreement to within some tolerance. In the absence of any definitive guide as to the likely precision of the data, we specify that the total simulated rainfall within a block must agree to within 1mm of that observed if under 10mm, and to with 10% if greater than 10mm. For completely dry blocks it is generally easy to generate points corresponding to exactly zero rainfall.

So for the Gibbs sampling, the full conditional distribution given by (3) must be restricted to the part of the distribution corresponds to a sufficiently close match for the total rainfall for that block. Therefore the required distribution is a truncated multivariate normal, given by (3), but truncated such that

$$\left| \sum_{a \in A} f^{-1}(y_a) - R \right| \leq d.$$

Here, $f^{-1}(y_a)$ is the rainfall corresponding to y_a, the simulated value of the latent GMRF at location a, and $f^{-1}(\cdot)$ is the appropriate quadratic root from the inverse transformation of (1):

$$f^{-1}(y_a) = \begin{cases} \left(\frac{\sqrt{{\alpha_1}^2 - 4\alpha_2(\alpha_0 - y_a)} - \alpha_1}{2\alpha_2} \right)^{1/\gamma} & \text{if } y > \alpha_0 \\ 0 & \text{otherwise.} \end{cases}$$

R is the total observed rainfall within that block:

$$R = \sum_{a \in A} r_a,$$

where r_a is the observed rainfall at location a. Finally, d is the discrepancy allowed between simulated and observed rainfall for that block:

$$d = \begin{cases} \max\left(100, \frac{R}{10}\right) & \text{if } R > 0, \\ 0 & \text{otherwise.} \end{cases}$$

Note that rainfall here is still in units of 1/100mm. We also note that the measurement error introduced here is not entirely consistent with the model — we return to this point in the discussion.

In order to generate a point from this truncated multivariate normal distribution, we simply generate points from the full distribution (3), and accept the first point to fall in the required region. Around 75% of blocks were matched exactly on the first attempt, dry blocks generally being easy to match, and another 14% within 10 attempts; approximately 0.1% needed more than 1000 attempts. Blocks in the added spatio-temporal border can be updated unconditionally from a single point generated from (3).

At this stage, it is worth noting why several ideas in the literature for improved efficiency of simulation from a GMRF were not used. Firstly, in problems with high correlation between locations, it is advantageous to update larger blocks of sites simultaneously (Knorr-Held and Rue, 2002) to gain better mixing and convergence in the Markov chain. Here however, at each update, the total rainfall in each 5×5 block must be consistent with the observed rainfall total for that block and therefore it is most natural and convenient to update blocks of this size at each step. This also has implications for use of the algorithms of Rue (2001) for fast simulation of GMRFs, the idea there being to order the locations such that the bandwidth of the precision matrix is minimised, then taking advantage of

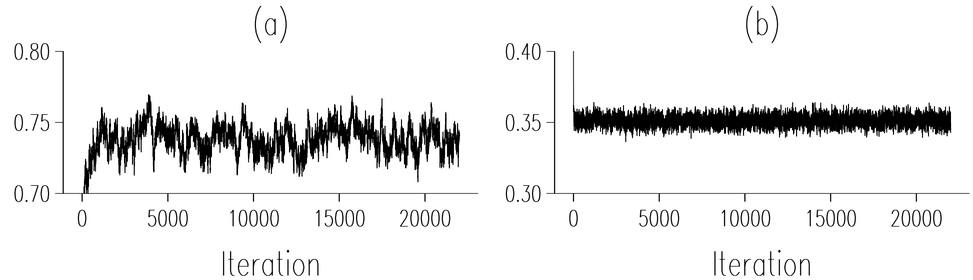

Fig. 6. Trace plots of (a) lag 1 correlation in time, (b) proportion of wet locations (fine scale) within wet blocks (coarse scale).

Table 3. Comparison of summary statistics of observed data with simulated realisations, averaged over 5000 realisations.

Statistic	*Observed*	*Simulated*
Propn wet locations	0.090	0.093
Propn wet locations within wet blocks	0.334	0.351
Propn correctly classified locations (wet/dry)	—	0.929
Propn correctly classified locations in wet blocks	—	0.739
Lag 1 correlation in space	0.906	0.905
Lag 1 correlation in time	0.704	0.739

computational routines for band-matrices. This can result in considerable computational gains when large blocks are being updated, but for the relatively small blocks we are dealing with here, the extra effort outweighs any computational gain.

Statistics were collected from each realisation and plots and tests of convergence were applied using CODA (Best et al., 1995). Here we report results from a run of 20000 iterations, after a burn-in of 2000, although shorter runs are probably adequate. Using Fortran 90 on a Sun Ultra2, each update took about 10 seconds of CPU time and therefore the full run reported here took around 60 hours. Fig. 6 shows the long-term behaviour of two of the summary statistics monitored, namely the correlation at a time lag of one hour and the proportion of wet locations within wet blocks. Similar plots were examined for the mean and variance of the latent Gaussian variable, other correlations in space and time and other proportions of wet and correctly classified (wet/dry) locations. Table 3 shows some summary statistics, illustrating the close agreement between the observed dataset and the simulated realisations and hence providing some sort of validation for our model.

Fig. 7 shows two simulated disaggregations. Comparison with the corresponding observed data in Fig. 1a shows the disaggregations to be similar in most respects to the original data. An overall proportion of correctly classified locations within wet squares of 74% (Table 3) compares favourably with the 65% reported by Mackay et al. (2001).

As a further model validation step, we should check our assumption of multivariate normality. The choice of transformation in Section 2.1 ensures a good fit for marginal (univariate) normality, but this does not automatically ensure multivariate normality of the latent variable. Fig. 8 therefore illustrates the bivariate distribution of the latent variable at a spatial lag of 1 at the fine scale (8km), for rain levels up to 50mm. Fig. 8(a) shows

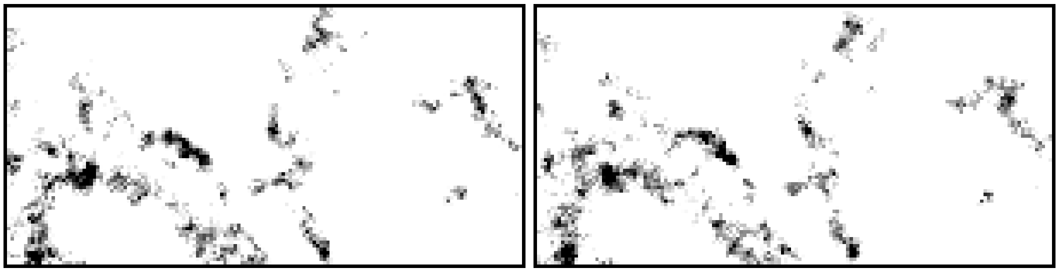

Fig. 7. Example disaggregations of the data from Fig. 1b. Rainfall intensities are displayed on the same scale as in Fig. 1.

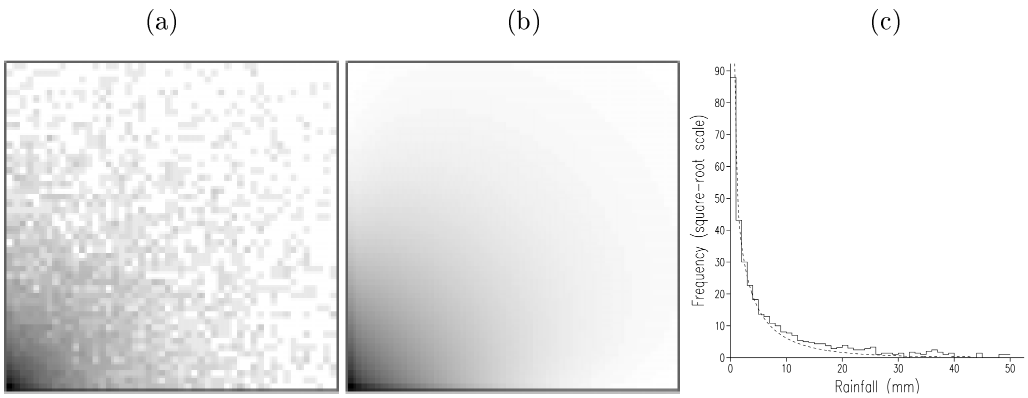

Fig. 8. Bivariate distribution of rainfall at a spatial lag of 1 at the fine scale (8km): (a) bivariate histogram of observed counts for pairs of wet locations (white indicates a zero count and increasingly dark squares represent larger counts); (b) bivariate histogram of expected counts for pairs of wet locations; (c) histogram of rainfall for locations for which the adjacent location was dry: observed (—), expected (- - -).

the empirical bivariate histogram of counts, and (b) the expected histogram, given the estimated correlation at that spatio-temporal lag, here $\hat{\rho}_{010} = 0.89$. Both of these only include the quadrant of the distribution corresponding to pairs of locations that are both wet, but (c) shows a plot of observed and expected counts for pairs of locations with one wet and the other dry. Finally, this bivariate normal distribution predicts that 86% of pairs of locations at this lag should both be dry, and we observed 89%. Therefore agreement can be seen to be generally good in all cases. Similar pictures were obtained for the bivariate distributions at other short lags.

4. Discussion

We have seen that we can successfully transform rainfall to a Gaussian variable and hence gain access to the existing methodologies for GMRFs, disaggregation then being straightforward and computationally feasible. One of the most attractive features of GMRFs is that such a good fit to the correlation structure can be obtained with a small neighbourhood and hence a relatively small number of parameters. We used a neighbourhood here of size

$5 \times 5 \times 3$, chosen empirically as the smallest size that gave an acceptable fit to the correlation structure of the data. The isotropy assumption also allows the number of parameters to be kept to a minimum and the results obtained can be seen visually to be acceptable. Further investigation would be useful to make formal comparisons of the efficiency of different neighbourhood sizes and ranges, extending the results in Rue and Tjelmeland (2002) to three dimensions.

We have demonstrated here that the modelling strategy works, the resulting realisations being convincingly close to the original data and visually much better than achieved previously. However, all our analysis was based entirely on the sequence of 12 hourly time points. A more rigorous approach, adopted by Chandler et al. (2000), would be to estimate model parameters from an independent, longer data sequence, e.g. for the same month in the previous year, and then use these parameters for the disaggregation. In general, data this similar might not even be available, so before practical application of this method, further work to assess the sensitivity of the results to changes in the model parameters would be useful. However, as we are conditioning on observed totals, we would not anticipate small changes in the GMRF parameters to have much effect on the results.

We pointed out earlier that the measurement error introduced in Section 3 is not entirely consistent with the model. If the errors at each location on the fine scale were independent, a spike would be expected in the correlation function at lag 0. We do not see this in Figure 4(a), and in practice probably wouldn't expect the errors to be white noise anyway, as they would more likely be spatially correlated. Noting the good agreement between the observed and predicted lag 1 correlation in Table 3, we tentatively conclude that not incorporating this measurement error in the model is not a major oversight.

Finally, we note that GMRF specification is convenient for conditional simulation, however the method is still computationally intensive. Further work therefore, to develop a more efficient methodology to simulate from a GMRF conditional on a non-linear system of equations being satisfied, would be useful.

Acknowledgements

Both authors acknowledge support from the Scottish Executive Environment and Rural Affairs Department. We also thank Richard Chandler, Håvard Rue, Tony Pettitt and Gavin Gibson for discussions on this work and the referees for their helpful suggestions.

References

Besag, J. and C. Kooperberg (1995). On conditional and intrinsic autoregressions. *Biometrika 82*, 733–746.

Best, N. G., M. K. Cowles, and S. K. Vines (1995). *CODA: Convergence Diagnostics and Output Analysis Software for Gibbs sampling output, Version 0.30.* Cambridge, UK: MRC Biostatistics Unit.

Chandler, R. E., N. G. Mackay, H. S. Wheater, and C. Onof (2000). Bayesian image analysis and the disaggregation of rainfall. *Journal of Atmospheric and Oceanic Technology 17*, 641–650.

Cressie, N. (1991). *Statistics for Spatial Data.* New York: Wiley.

Durban, M. and C. A. Glasbey (2001). Weather modelling using a multivariate latent Gaussian model. *Agricultural and Forest Meteorology 109*, 187–201.

Glasbey, C. A. and I. M. Nevison (1997). Rainfall modelling using a latent Gaussian variable. In T. G. Gregoire et. al. (Ed.), *Modelling Longitudinal and Spatially Correlated Data: Methods, Applications, and Future Directions*, Number 122 in Lecture Notes in Statistics, pp. 233–242. Springer, New York.

Guillot, G. (1999). Approximation of Sahelian rainfall fields with meta-Gaussian random functions. Part 1: model definition and methodology. *Stochastic Environmental Research and Risk Assessment 13*, 100–112.

Hughes, J. P., P. Guttorp, and S. P. Charles (1999). A non-homogeneous hidden Markov model for precipitation occurrence. *Applied Statistics 48*, 15–30.

Knorr-Held, L. and H. Rue (2002). On block updating in Markov random field models for disease mapping. *Scandinavian Journal of Statistics 29*, 597–614.

Mackay, N. G., R. E. Chandler, C. Onof, and H. S. Wheater (2001). Disaggregation of spatial rainfall fields for hydrological modelling. *Hydrology and Earth System Sciences 5*, 165–173.

Mardia, K. V., C. Goodall, E. J. Redfern, and F. J. Alonso (1998). The Kriged Kalman filter (with discussion). *Test 7*, 217–285.

Pfeifer, P. E. and S. J. Deutsch (1980). A three-stage iterative procedure for space-time modeling. *Technometrics 22*, 35–47.

Rodriguez-Iturbe, I., D. R. Cox, and V. Isham (1988). A point process model for rainfall: further developments. *Proceedings of the Royal Society of London, Series A 417*, 283–298.

Rue, H. (2001). Fast sampling of Gaussian Markov random fields. *Journal of the Royal Statistical Society, Series B 63*, 325–338.

Rue, H. and H. Tjelmeland (2002). Fitting Gaussian Markov random fields to Gaussian fields. *Scandinavian Journal of Statistics 29*, 31–49.

Sansó, B. and L. Guenni (1999). Venezuelan rainfall data analysed by using a Bayesian space-time model. *Applied Statistics 48*, 345–362.

Stern, R. D. and R. Coe (1984). A model fitting analysis of daily rainfall data (with discussion). *Journal of the Royal Statistical Society, Series A 147*, 1–34.

Wikle, C. K., R. F. Milliff, D. Nychka, and L. M. Berliner (2001). Spatiotemporal hierarchical Bayesian modeling: Tropical ocean surface winds. *Journal of the American Statistical Association 96*, 382–397.